

Microbial Communities Collectively Recycle Cadavers Over One Year of Human Decomposition

Allison R. Mason¹, Lois S. Taylor², Naomi E. Gilbert¹,
Steven W. Wilhelm¹, Jennifer M. DeBruyn^{1,2*}

¹Department of Microbiology, University of Tennessee-Knoxville, 1311
Cumberland Avenue, Knoxville, 37996.

²Department of Biosystems Engineering and Soil Science, University of
Tennessee-Knoxville, 2506 E.J. Chapman Drive, Knoxville, 37996.

*Corresponding author(s). E-mail(s): jdebruyn@utk.edu;

Abstract

During terrestrial vertebrate decomposition, host and environmental microbial communities work together to drive biogeochemical cycling of carbon and nutrients. These mixed communities undergo dramatic restructuring in the resulting decomposition hotspots. To reveal the succession of both the active microbial members and the metabolic pathways they use, we generated metatranscriptomes from soil samples collected over one year from below three decomposing human bodies. Soil microbes increased expression of heat shock proteins in response to decomposition products changing physiochemical conditions (*i.e.*, reduced oxygen, high salt). Increased fungal lipase expression implicated fungi as key decomposers of fat tissue. Expression of nitrogen cycling genes was phased with soil oxygen concentrations: during hypoxic soil conditions, genes catalyzing N-reducing processes (*e.g.*, hydroxylamine to nitric oxide and nitrous oxide to nitrogen gas during reduced oxygen conditions) were increased, followed by increased expression of nitrification genes once oxygen diffused back into the soil. Increased expression of bile salt hydrolases implicated a microbial source for

the high concentrations of taurine typically observed during vertebrate decomposition. Collectively, microbial gene expression profiles remained altered even after one year. Together, we show how human decomposition alters soil microbial gene expression, revealing both ephemeral and lasting effects on soil microbial communities.

Keywords: Human Decomposition, Microbial Succession, Metatranscriptomics, Soil Microbial Ecology

Introduction

Soil microbial communities are important drivers of ecosystem processes in terrestrial environments. Many soil microbes are decomposers that degrade complex organic matter and drive nutrient cycling in terrestrial ecosystems. Environmental disturbances can impact the presence and/or activity of soil microorganisms involved in these cycles, ultimately affecting nutrient availability and greenhouse gas emissions, such as CO₂ and N₂O [1, 2]. Vertebrate death and subsequent carcass deposition in terrestrial ecosystems is one disturbance resulting in the deposition of large quantities of organic C and N [3–10], along with other elements (P, K, S, *etc.*) [11], which collectively stimulate microbially-mediated biogeochemical cycling. In addition to this, changes in pH, temperature, and fluctuations in soil oxygen provide abiotic filtering further impacting microbial metabolic strategies [7–9, 11–13]. Vertebrate decomposition also results in mixing of host and environmental microbes: the animal’s microflora are flushed into the soil along with decomposition products where they further contribute to decomposition processes (*e.g.*, organic nitrogen mineralization) [14].

While C and N transformations have been documented during decomposition, the functional response of microbes and their roles in nutrient cycles remain unclear. The composition and structure of decomposition-impacted soil microbial communities have been investigated using sequencing of marker genes amplicons (*i.e.*, 16S rRNA, 18S

rRNA, ITS). This has allowed for the identification of changes in microbial biodiversity and taxonomic succession in response to vertebrate decomposition, revealing patterns that include increases in the anaerobic taxa *Firmicutes* and *Bacteroidetes* [15]. However, few studies have integrated soil biogeochemistry with microbial community composition, which can further help to describe microbial ecology in these decomposition systems. Taylor et al. (2024) [13] showed that fungal community shifts were linked to changes in soil dissolved oxygen, highlighting interactions between soil microbes and changes in the surrounding environment. While insightful for making potential connections between taxa and environment, these analyses do not inform which taxa are active members of the community, which functional pathways/genes are expressed, and how these pathways facilitate decomposition processes.

RNA sequencing (*i.e.*, metatranscriptomics) and metabolomics can be used to investigate microbial community functional succession during decomposition. They can identify how ecological functions, including C and N cycling, are impacted by decomposition events in terrestrial ecosystems. To date, applications of metatranscriptomics to vertebrate decomposition samples have been limited to internal host communities [16, 17]: Burcham et al. (2019) [16] revealed differential expression of amino acid and carbohydrate metabolism in the heart during mouse decomposition, while Ashe et al. (2021) [17] documented taxonomic shifts in gene expression of oral microbial communities during human decomposition.

We expected that the impacted soil microbial community, which includes a mix of host and environmental taxa, would also have altered gene expression profiles, given the release of decomposition byproducts into the soil during terrestrial decomposition. We previously assessed the decomposition-impacted soil metabolome [18], demonstrating a prevalence of amino acids and suggesting upregulation of organic nitrogen metabolic pathways. Additionally, DeBruyn et al. (2021) [18] showed the soil metabolome was

139 surprisingly still altered compared to starting conditions at the end of that 21-week
 140 study, suggesting long-term impacts of decomposition on soil microbial functioning.
 141
 142 Here, we investigated soil microbial gene expression during a one-year period of human
 143 decomposition. The overarching goal of this work was to assess the effects of vertebrate
 144 decomposition on ecosystem function by characterizing community-level shifts in soil
 145 microbial function. We hypothesized that: (i) gene expression would shift over time as
 146 resources were consumed and transformed and soil chemical and physical conditions
 147 changed due to the influx of decomposition products during soft tissue degradation
 148 [8, 9, 18]; (ii) gene expression for enzymes involved in nitrogen cycling would be altered,
 149 as changes in nitrogen pools have been previously described in decomposition soils [8];
 150 (iii) expression of genes involved in lipid metabolism would increase, as lipids from
 151 the body entered the soil during decomposition and previous studies identified lipoly-
 152 tic organisms in decomposition soils [12, 19]; (iv) microbial expression profiles in the
 153 impacted soil would not fully recover and remain altered even after a year, as previ-
 154 ous studies have shown that community composition was still altered at least a year
 155 after decomposition began [20, 21]. We analyzed metatranscriptomes of soil samples
 156 collected at six key timepoints over one year of human decomposition to determine
 157 the identity of active populations and the expression of genes and pathways relevant
 158 to the enhanced biogeochemical cycling observed in decomposition hotspots. We com-
 159 pared gene expression between decomposition timepoints and control soils that were
 160 unexposed to decomposition products to identify functions or functional pathways
 161 of interest. We show: (i) decomposition shifts soil microbial community gene expres-
 162 sion, with the effects still measurable after one year; (ii) expression of genes related to
 163 stress response are elevated in decomposition soils; (iii) expression of genes encoding
 164 triacylglycerol lipase differed between fungi (increased) and bacteria (decreased), indi-
 165 cating differential responses between bacterial and fungal decomposers; (iv) evidence
 166 for phased nitrification and denitrification, driven by changes in soil dissolved oxygen;
 167
 168
 169
 170
 171
 172
 173
 174
 175
 176
 177
 178
 179
 180
 181
 182
 183
 184

(v) evidence for organic sulfur processing (taurine) via bile salt hydrolases. This direct assessment of function expands the fundamental understanding of terrestrial vertebrate decomposition, providing insight into pathways of biogeochemical cycling within these hotspots.

Results

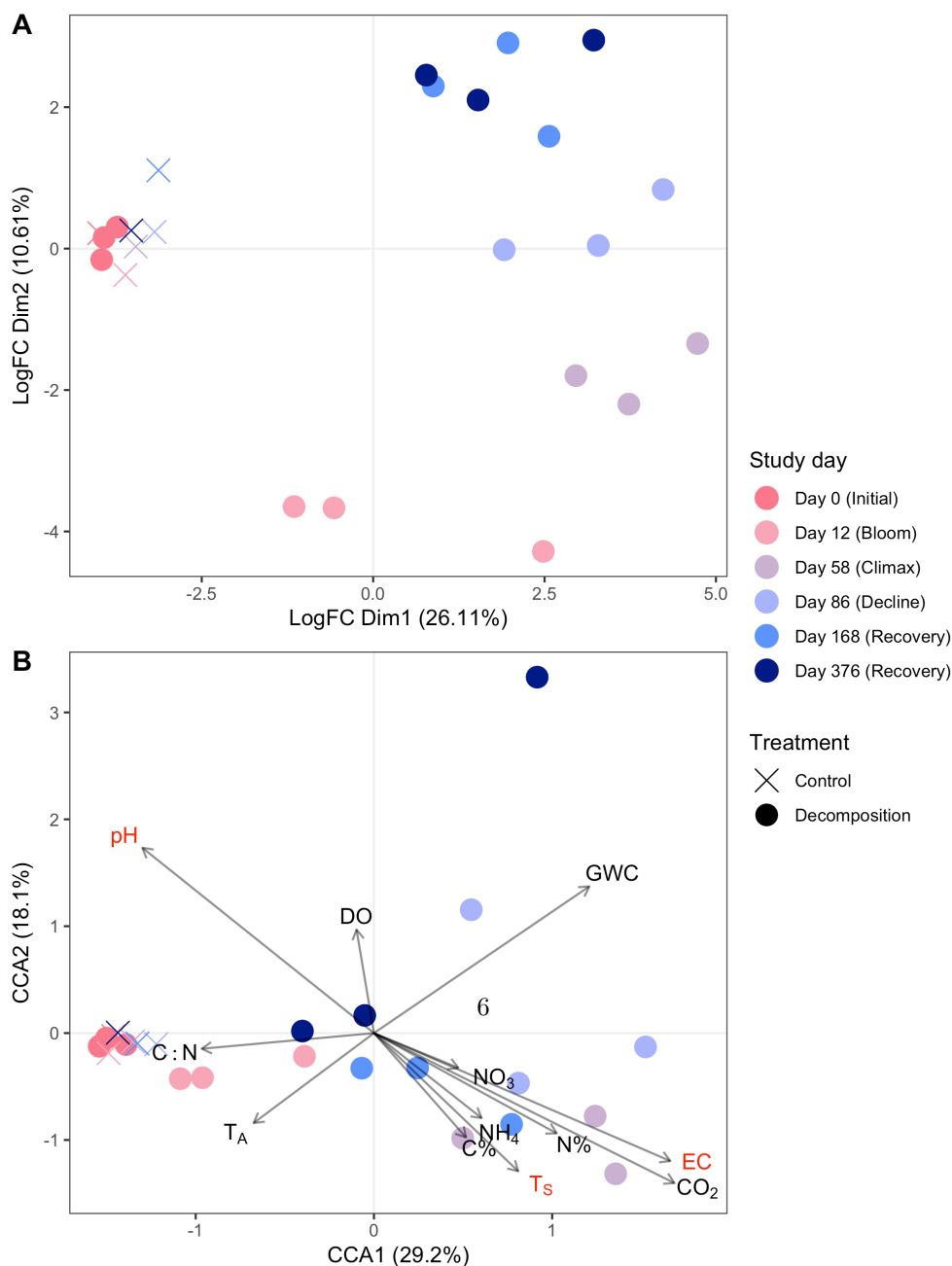
Soil Physiochemistry

Soil chemistry was altered in response to the presence of decomposing human cadavers, with multiple parameters still impacted after one year [13]. Generally, soil pH decreased and remained low in decomposition soils. Soil electrical conductivity (EC) increased in response to decomposition, remaining elevated through approximately day 58 before gradually decreasing throughout the remainder of the study (Fig. S1). Respiration (evolved CO₂) increased by an order of magnitude beginning at day 12, which corresponded to a reduction in soil dissolved oxygen (DO) to 29% - 48.9%. Ammonium concentrations increased 78-fold, reaching maximum concentrations between days 12 and 58. This was followed by decreased ammonium and increased nitrate concentrations at day 86, with nitrate concentrations reaching a maximum at day 168 (Fig. S1).

Microbial gene expression in response to human decomposition

Gene expression profiles in decomposition-impacted soils shifted away from controls and day zero samples as decomposition progressed (Fig 1A). Expression was most different from controls on study days 58, 86, 168 (Fig. S2), before starting to return toward control conditions on study day 376. After one year of decomposition, soil gene expression profiles had not returned to pre-decomposition conditions, as evidenced by their clustering away from controls and day zero samples in the MDS plot (Fig 1A).

Figure 1: Microbial gene expression profiles are altered during human decomposition. Multidimensional scaling (MDS) shows gene expression within soils changed as decomposition progressed (A). Canonical correspondence analysis (CCA) shows that environmental variables explained 47.3% of the variation in gene expression profiles (B). Variables in bold red type significantly ($p < 0.05$) explained some of the variation in gene expression profiles as assessed by Permutational Analysis of Variance (PERMANOVA). In both panels, treatment (control, decomposition) is denoted by shape, while color represents study day with associated decomposition phase (Fig. S5) in parentheses. In B, soil physiochemical variable loadings are represented by arrows: Gravimetric water content (GWC), electrical conductivity (EC), pH (pH), dissolved oxygen (DO), respiration (evolved CO_2 $\mu\text{mol gdw}^{-1}$), ammonium (NH_4), and nitrate (NO_3) concentrations (mg gdw^{-1}), percent carbon (%C), percent nitrogen (%N), carbon:nitrogen ratio (C:N), ambient temperature (T_A), and soil temperature (T_S).

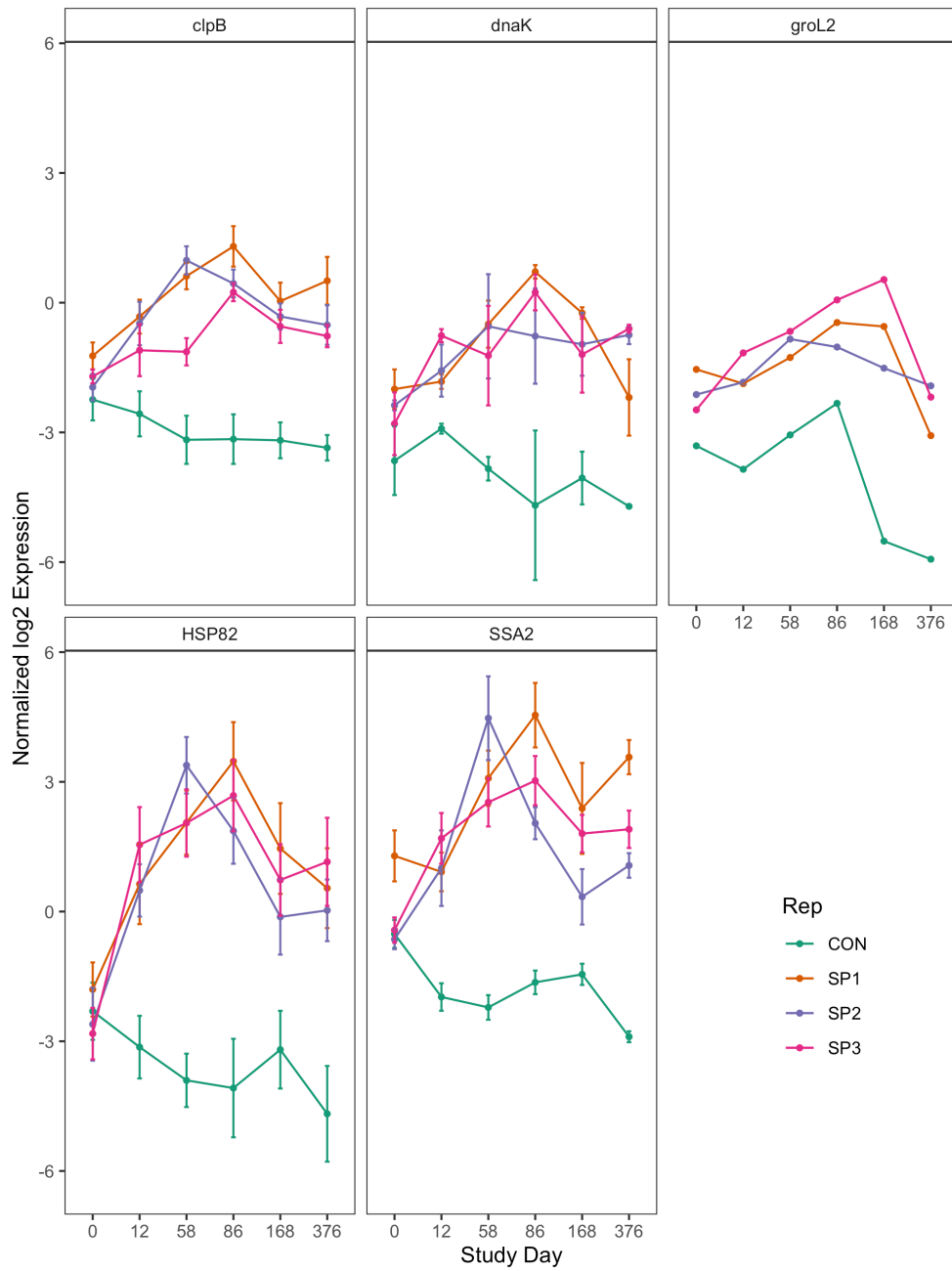


Some correlations were observed between gene expression shifts and soil physiochemical data at decomposition timepoints. Canonical correspondence analysis (CCA) was used to constrain gene expression data with soil physiochemical data (Fig 1B). CCA1 and CCA2 explained 29.2% and 18.1% of the variance in gene expression, respectively. Transcript profiles at day 12 were associated with an increase in soil carbon to nitrogen ratio (C:N). Gene expression profiles at days 58 to 86 were positively correlated with increased soil temperature, EC, and evolved CO₂, while study day 168 was associated with elevated levels of soil NO₃. Further, Permutational Analysis of Variance (PERMANOVA) revealed that internal accumulated degree hours (ADH) ($p = 0.001$), soil temperature ($p = 0.039$), pH ($p = 0.033$), and EC ($p = 0.031$) significantly explained some of the variation in gene expression profiles ($p < 0.05$). No other soil chemical variables were significant at $\alpha = 0.05$ (Table S1).

Overall, decomposition changed soil gene expression profiles over the one-year study relative to control soils. Differential expression analysis between decomposition and control soils identified 7,047 down-regulated and 38,425 up-regulated genes. Gene transcripts that were associated with control soils belonged to a wide variety of clusters of orthologous genes (COG) functional categories. Specifically, the top 20 genes whose expression was higher in control soils belonged to ten unique COG categories, including signal transduction mechanisms, transcription, and those of unknown function. In contrast, the top 20 genes whose expression was higher in decomposition soils only fell into four COG categories (Fig. S3 A): 1) post-translational modification, protein turnover, and chaperones; 2) energy production and conversion; 3) cell motility; and 4) carbohydrate transport and metabolism. The most common COG category represented in decomposition soils (80% of the top 20 genes) was post-translational modification, protein turnover, and chaperones. Within this category, several heat shock stress response genes were identified, including clpB, dnaK, groL2, SSA2, HSP82, and clpB (Table S2). Further investigation of these genes over time

shows that their expression increased, typically reaching maximum transcript levels around study days 58 and 86 (Fig 2). This corresponded to elevated soil temperatures below decomposing bodies between study days 12-80, with soil temperatures increasing to approximately 43°C [13], as well as maximum soil EC and minimum dissolved oxygen measurements between days 12 and 58 (Fig. S1).

Figure 2: Mean normalized log2 expression of heat shock proteins identified by differential expression analysis comparing decomposition and control soils. Each panel represents a single heat shock gene, labeled with gene names, identified via Prodigal. Symbol color denotes if the sample is a control (CON, green), or one of three individuals: SP1 (orange), SP2 (purple), or SP3 (pink). Error bars are standard error of individual query genes in the top 20 transcripts associated with decomposition soils.



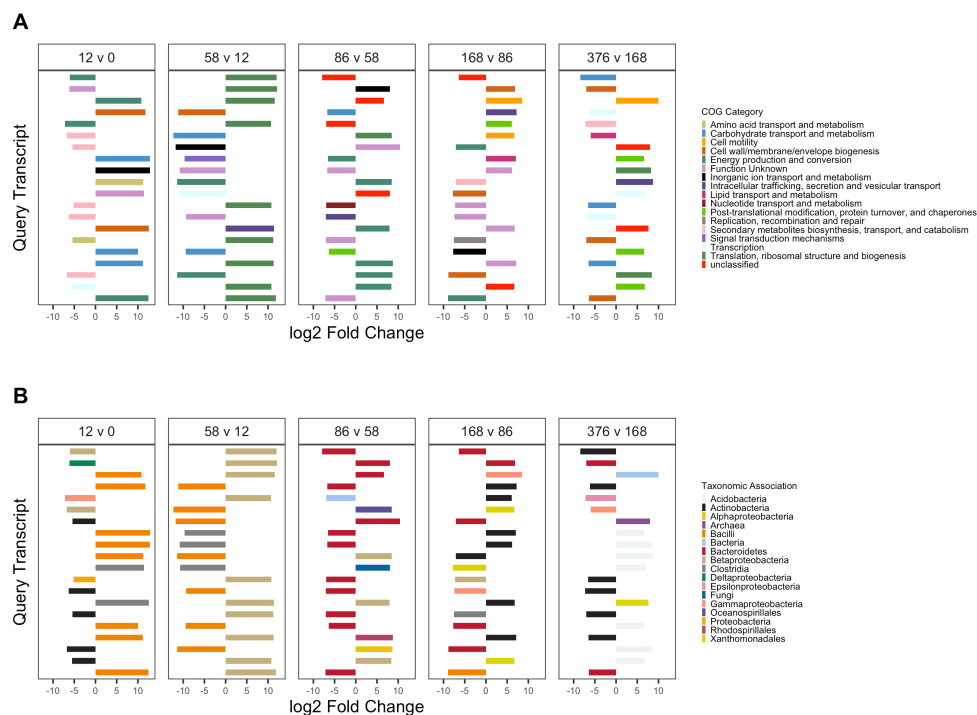
Taxonomy associated with top differentially expressed gene transcripts also differed between control and decomposition soils. The top 40 most significant differentially

expressed gene transcripts in decomposition soils were associated with Fungi, *Actinobacteria*, and *Xanthomonadales*, while gene transcripts in controls were associated with *Acidobacteria*, *Cyanobacteria*, *Proteobacteria* (α , δ , γ), and *Planctomycetes* (Fig. S3 B). The greatest number of differentially expressed genes relative to control samples was observed at day 86, where we saw 145,460 and 124,883 up- and down-regulated genes, respectively.

Temporal gene expression shows shifted decomposer functions

Differential expression analysis between sequential study days revealed which genes were altered during decomposition. The top ten transcripts that changed in representation (increased/decreased), determined by the lowest p-values from differential expression analysis, are reported in Table S3 and Fig 3.

Figure 3: Top twenty up- and down-regulated genes in decomposition soils comparing sequential study days (0, 12, 58, 86, 168, 376) colored by COG functional category (A) and taxonomic annotation (B). Positive values denote increased expression compared to the preceding timepoint, while negative values denote a decrease.



Expression of genes annotated with the COG categories cell wall/membrane/envelope biogenesis, inorganic ion transport and metabolism, and carbohydrate transport and metabolism increased proportionally from day 0 to 12. In contrast, expression of secondary metabolite biosynthesis, transport, and catabolism genes decreased during this period (Fig 3A). Transcripts from *Bacilli* and *Clostridia* increased, while transcripts from *Actinobacteria* decreased between study days zero and 12 (Fig 3).

Between days 12 and 58, 90% of the top 10 upregulated genes were associated with the translation, ribosomal structure and biogenesis COG and all were taxonomically associated with *Betaproteobacteria* (Fig 3A,B). Many of these genes were annotated as ribosomal protein large (RPL), involved in ribosomal binding. Genes across multiple COG categories with taxonomic associations to *Bacilli* and *Clostridia* decreased

507 between study days 12 and 58, six of which were transcripts that previously increased
508
509 between days zero and 12 (Fig 3B, Table S3).

510
511 Multiple transcripts associated with the energy production and conversion COG, as
512
513 well as transcripts annotated as inorganic transport and metabolism, and transla-
514
515 tion, ribosomal structure and biogenesis, increased between days 58 and 86 (Fig 3A).
516 Two of the upregulated energy and production and conservation transcripts were
517
518 associated with cytochrome c oxidase subunits in *Betaproteobacteria*, while another
519
520 was annotated as *hao*, encoding the enzyme hydroxylamine dehydrogenase which is
521
522 involved in conversion of hydroxylamine to nitrite during nitrification (Table S3). Fur-
523
524 ther investigation into hydroxylamine dehydrogenase showed a significant increase in
525
526 *hao* transcripts at day 86 followed by subsequent decreases at days 168 and 376 (F
527
528 = 4.183; $p = 0.02$). This increase corresponded to decreased soil ammonium levels
529
530 and subsequent accumulation of nitrate (Fig. S1). Half of the 10 most downregulated
531
532 genes between days 58 and 86 were not assigned to a COG (*i.e.*, unclassified) or were
533
534 of unknown function.

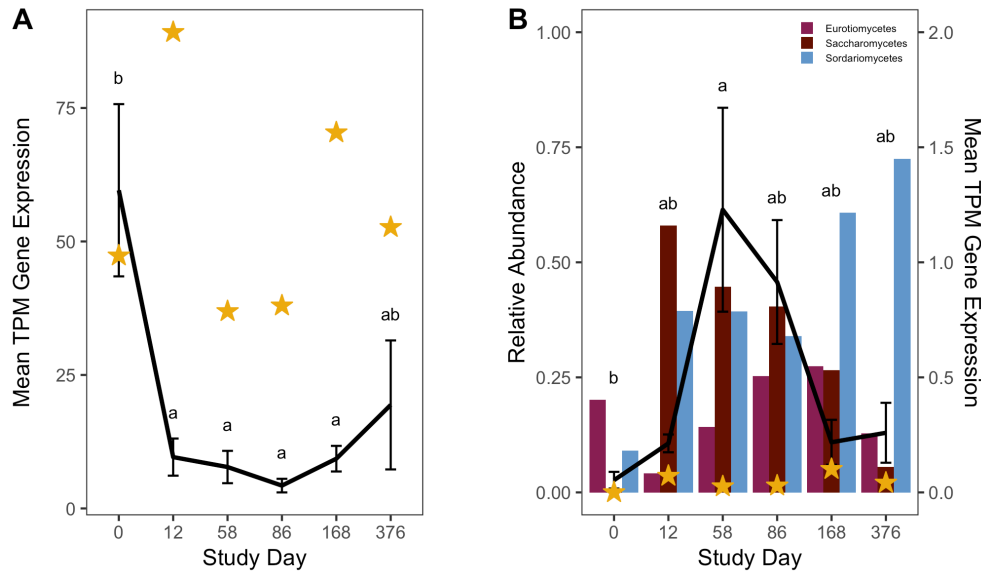
535
536 Differential expression comparing study days 86 with 168 and 168 with 376 identified
537
538 genes across a variety of functional categories, with many unclassified in the COG
539
540 database or with unknown function (Fig 3A). Expression of carbohydrate transport
541
542 and metabolism genes associated with *Bacilli* decreased between day 168 and 376.
543
544 *Acidobacteria* transcripts increased in decomposition-impacted soils between study
545
546 day 168 and 376, but were not associated with any single COG category (Fig 3B).

545 **Organic carbon metabolism**

546
547 We expected to observe increased expression of lipid metabolizing genes during active
548
549 and advanced decomposition as microbes degraded lipids deposited in the soil [19].
550
551
552

Therefore, we investigated changes in triacylglycerol lipase (enzyme commission number: 3.1.1.3) gene transcription in our soils. Generally, lipase transcripts decreased as decomposition progressed (HLM $F = 6.564$, $p < 0.001$), however we also observed a significant interaction between study day and taxonomic annotation ($F = 8.786$; $p < 0.001$). Specifically, lipase gene transcripts annotated as bacteria decreased with decomposition time ($F = 10.392$; $p = 0.001$), while fungal lipase transcripts increased, reaching a maximum at study day 58 ($F = 4.509$; $p = 0.015$) (Fig 4).

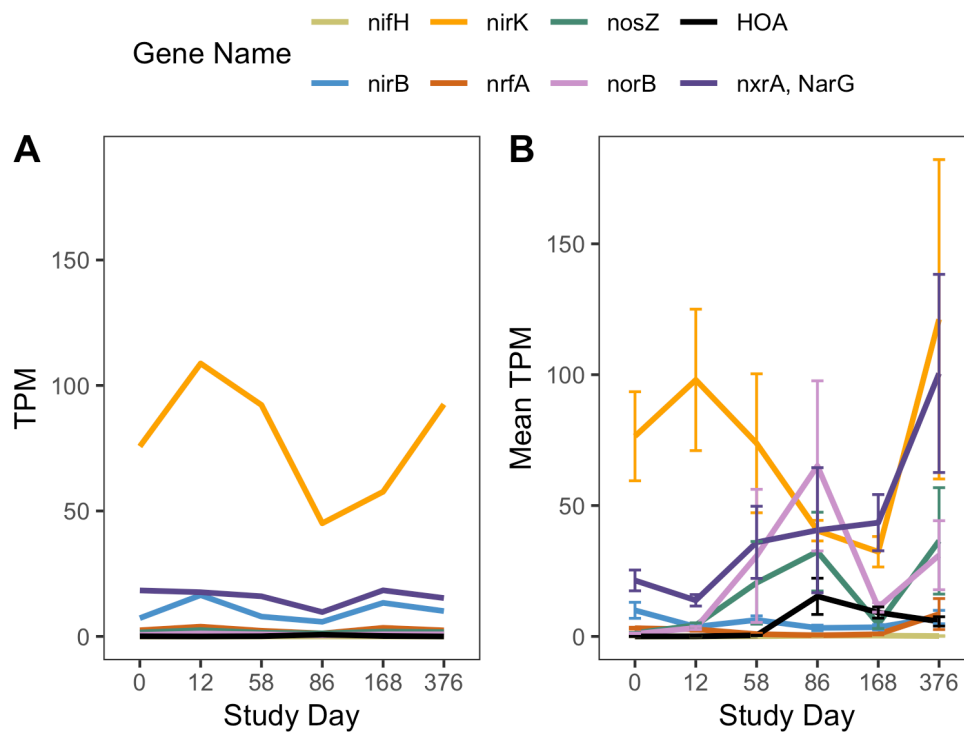
Figure 4: Mean transcript abundance, in transcripts per million (TPM), of all bacterial (A) and fungal (B) triacylglycerol lipase (EC 3.1.1.3) genes over time. Abundance of both bacterial ($p = 0.001$) and fungal ($p = 0.015$) lipase transcripts change significantly over time. Black lines (A, B) report mean and standard deviation of TPM from three individuals (black line), while gold stars denote mean TPM in control soils. Letters are the result of post-hoc Tukey tests between decomposition timepoints. In B, bars show the relative abundance of the fungal classes *Saccharomycetes*, *Sordariomycetes*, and *Eurotiomycetes*, reported in Taylor et al. (2024).



Nitrogen- and sulfur compound transformations

Expression of nitrogen cycling genes was impacted in response to human decomposition. Due to the detection of hydroxylamine oxidoreductase (*hao*) transcripts in our differential expression analysis, and our hypotheses predicting changes to nitrogen transformation processes, the expression of genes encoding common enzymes involved in nitrogen cycling (*nifH*, *nirB*, *nirK*, *norB*, *nosZ*, *nrfA*, *nxrA*, and *amoA*) were assessed using their enzyme commission numbers (Fig 5A,B). *nifH*, encoding a subunit of nitrogenase which is involved in nitrogen fixation, displayed little to no changes in gene expression between control and decomposition soils. Transcripts for two genes encoding enzymes contributing to the last two steps of denitrification, *norB* (nitric oxide reductase) and *nosZ* (nitrous oxide reductase), increased between study days 12 and 86, and decreased at study day 168 before increasing again at day 376. In contrast, expression of genes encoding nitrate reductase, *narG*, and NO-forming nitrite reductase, *nirK*, remained low until day 376 when transcripts for both genes increased. As noted above, expression of *hao*, encoding hydroxylamine dehydrogenase, increased at study day 86 before decreasing at remaining timepoints (Fig 3A, Fig 5B). Expression of *amoA*, encoding a subunit of ammonia monooxygenase, and *nxrA*, encoding a subunit of nitrite oxidoreductase, which are involved in nitrification, changed in response to decomposition. *amoA* transcripts initially decreased at day 12, remaining reduced until study day 376. Similarly, abundance of transcripts encoding enzymes involved in dissimilatory nitrate reduction, *nirB*, and *nrfA*, was low for the first 168 days, with *nrfA* expression increasing at day 376 (Fig 5B).

Figure 5: Mean gene expression, in transcripts per million (TPM), of commonly used marker genes for enzymes involved in nitrogen cycling over time in controls (A) and decomposition (B) soils. Data in B represent mean and standard deviation of TPM from three individuals.

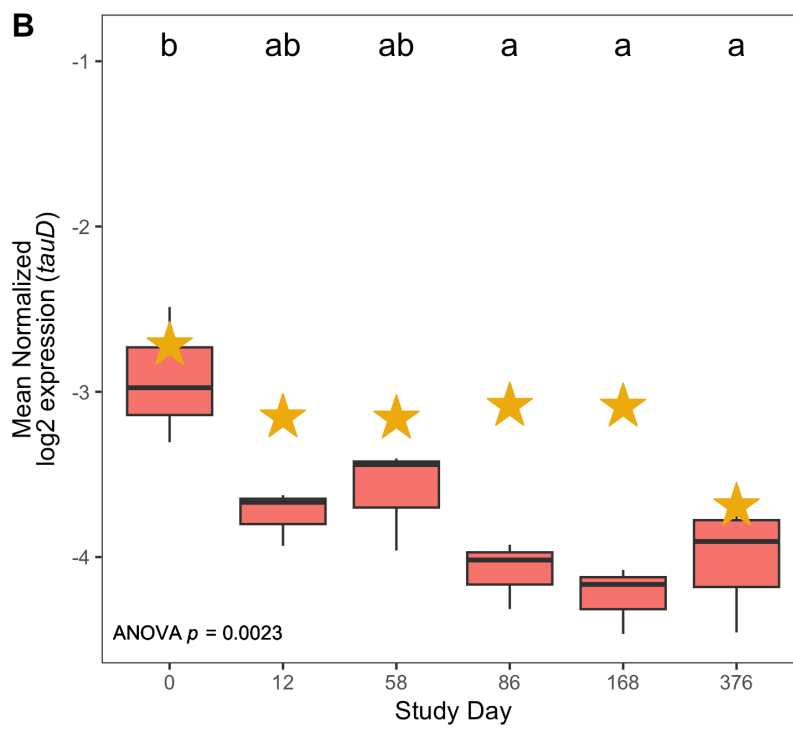
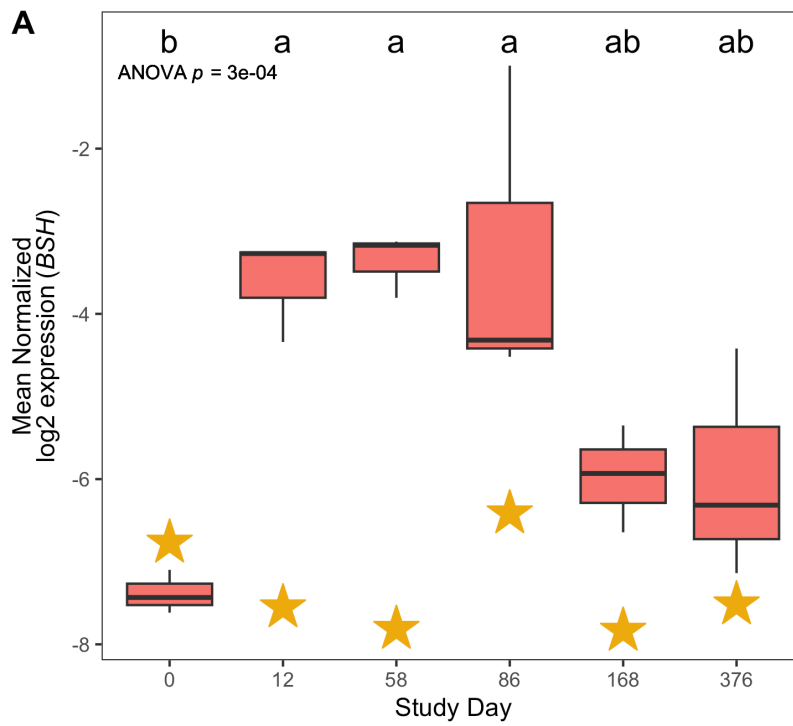


Expression of genes involved in metabolism of nitrogen and sulfur-containing compounds were also impacted by human decomposition. Specifically, four of the top ten genes whose expression decreased at day 12 were related to taurine metabolism, with their annotations associated with *tauD*, encoding taurine dioxygenase. (Table S3). Further investigation into *tauD* showed that mean expression of these genes decreased steadily over one year, beginning at day 12 (Fig 6B); however, *tauD* expression in response to human decomposition was variable across taxonomic associations. Most *tauD* transcripts were associated with *Gammaproteobacteria*, *Actinobacteria*, *Betaproteobacteria*, *Alphaproteobacteria*, and fungi. While a majority of the *tauD* gene queries displayed reduced expression over time, expression of fungal-associated and a few *Betaproteobacteria*-associated *tauD* genes increased at day 58 (Fig. S4). Sources of taurine in the human body include taurine absorbed from the diet and taurine produced

691 from anaerobic microbial deconjugation of bile salts via bile salt hydrolase (BSH)
692 enzymes [22]. Therefore, we examined transcripts encoding BSH enzymes in decom-
693 position soils. Expression of these genes was elevated at days 12, 58, and 86 before
694 converging toward pre-decomposition levels at days 168 and 376 (Fig 6A). Hierarchi-
695 cal liner mixed effects (HLM) models showed that both *tauD* (HLM $F = 7.356$, $p =$
696 0.002) and BSH ($F = 13.768$, $p < 0.001$) gene expression was significantly different
697 over time (Fig 6A,B).
701

702
703
704 **Figure 6: Mean bile salt hydrolase, BSH, (A) and *tauD*, taurine dioxy-**
705 **genase, (B) log2 normalized expression in controls (gold stars) and**
706 **decomposition (boxplots) soils.** Boxplots display the 25th and 75th quartiles
707 and median log2 normalized values between all three individuals at each timepoint.
708 ANOVA p-value is the result of a hierarchical linear mixed effects model accounting
709 for repeated measures of each donor block, while letters denote the results of *post-hoc*
710 Tukey test.

711
712
713
714
715
716
717
718
719
720
721
722
723
724
725
726
727
728
729
730
731
732
733
734
735
736



Discussion

The goal of this study was to assess microbial gene expression in soils responding to human decomposition. Metatranscriptomics were applied to soil samples collected over one year from below three decomposing human bodies. From this, we found that microbial gene expression reproducibly shifted over time. Additionally, we showed that gene expression profiles had not recovered to pre-decomposition conditions after one year. Comparison of control and decomposition expression profiles revealed that heat-shock proteins were elevated in response to decomposition. We also described expression patterns between decomposition timepoints, noting changes in functional gene categories at certain timepoints, in particular with respect to lipid, nitrogen and sulfur metabolism.

Decomposition impacted soil community gene expression for at least one year

Gene expression profiles remained altered after one year of decomposition. It is unclear if soil microbial communities, in terms of gene expression profiles, had reached a new steady state as a result of decomposition, or if they would eventually return to pre-decomposition conditions. The soil pH, EC, NH_4^+ , NO_3^- , and total nitrogen (TN) exhibited differences (although not statistically significant) in these soils following a year of decomposition, however bacterial and fungal community structures, as assessed by rRNA amplicon libraries, were still altered [13]. This indicates that decomposition can continue to structure microbial communities and impact their function for extended periods of time. While nutrient pools and communities both demonstrate less rapid change at later time points in the study, there is no evidence suggesting an arrival at a steady-state post-disturbance microbial community within our study. In some studies, human decomposition can result in elevated carbon and nutrients (organic nitrogen, ammonium, nitrate, and phosphate) for longer than a year [3], suggesting

decomposition events have long-lasting effects on the local ecosystem. Together, this has implications for terrestrial ecosystem processing (*e.g.*, nutrient cycling, emission of greenhouse gasses, etc.), as we show that decomposition alters functional metabolism pathways within soil microbial communities. It is clear that extended sample collections beyond a single year are needed to address how long microbial communities are affected, and whether there is a return to the original state or some new altered community condition.

Bacteria, fungi, and archaea were all represented by expressed genes throughout decomposition, suggesting that members of all three domains have the potential to contribute to decomposition processes and nutrient cycling. While a majority of annotated transcripts were identified as bacterial, fungal transcripts were the second most abundant group. Fungal transcripts made up almost half (*e.g.*, seven of the top fifteen) of the significantly differentially expressed genes associated with decomposition-impacted soils. Additionally, with respect to expression shifts between decomposition timepoints, fungal transcripts were among the topmost upregulated genes at study day 86. This is not surprising as fungi are key decomposers, involved in the degradation of organic matter in terrestrial ecosystems [23]. It was interesting to see an increase in certain fungal transcripts, such as lipase, at study days 58 and 86 when soil oxygen began to recover. We would expect lipids to enter the soil as tissues are broken down during decomposition, so we were surprised to see bacterial lipase genes decrease during decomposition. This suggests that microbial activity in decomposition soils may be constrained by the changing chemical environment, potentially altered oxygen levels in the case of bacterial lipase gene expression. Prior work with these same soils showed that soil oxygen concentration was a key driver of changes in both bacterial and fungal community composition [13].

875 **Increased stress response during decomposition**

876

877 Soil microbial communities expressed stress response genes in response to human
878 decomposition. Differential expression analysis identified increased expression of mul-
879 tiple heat shock proteins associated with the taxa *Xanthomonadales*, *Actinobacteria*,
880 and fungi. Upon further investigation, expression of these genes increased through day
881 58 and remained high for the remainder of the year. Soil temperature was elevated rel-
882 ative to controls between study days 8 and 80, with maximum temperatures $>40^{\circ}\text{C}$,
883 while soil electrical conductivity increased up to $663\ \mu\text{S cm}^{-1}$ (16X higher than back-
884 ground) through day 58 before slowly decreasing through the remainder of the study.
885 Soil electrical conductivity correlates with ionic strength and can be an indicator
886 of increased salinity [24]. During vertebrate decomposition, elevated conductivity in
887 impacted soils is attributable to sodium (Na), potassium (K), and ammonium (NH_4)
888 [8–11, 13]. As a result, we would expect these microbes to be experiencing both heat
889 and osmotic stress during this period. Prior work has observed increased heat shock
890 gene expression during salt stress in paddy soils [25] and the presence of both heat
891 and osmotic stress genes in desert soils along a salt gradient [26], suggesting saline
892 conditions can alter the expression of heat and/or osmotic stress genes. In our study
893 we observed the stress response within soil microbial communities was stimulated dur-
894 ing human decomposition. At this time, however, it is unclear if expression of these
895 genes is in response to heat stress alone, or in combination with osmotic stress.

908

909 **Increased expression of fungal lipase genes during**

910

911 **decomposition**

912

913 Human fat tissue contains lipids that are broken down during decomposition. There-
914 fore, we assessed expression of triacylglycerol lipase genes in decomposition soils. Our
915 results show that expression of triacylglycerol lipase genes was altered in response
916 to decomposition, and these shifts differed between bacterial and fungal transcripts.

917

Specifically, bacterial triacylglycerol lipase transcripts decreased in response to decomposition, while fungal triacylglycerol lipase transcripts increased. Further, expression of these genes corresponded to changes in relative abundance of the fungal classes *Saccharomycetes*, *Sordariomycetes*, and *Eurotiomycetes* [13]. These fungi have been previously associated with decomposition soils [27, 28] and are known to contain triacylglycerol lipase genes in their genomes [29, 30], suggesting that they play a role in lipid degradation in decomposition soils.

Our observation of an overall decrease in triacylglycerol lipase transcripts contrasts with previous work by Howard et al. (2010) [19], who observed increased copies of Group 1 lipase genes via qPCR during swine (*Sus scrofa*) decomposition. Fatty acid composition differs between human and pig tissue [31], potentially altering the lipid profile available for microbes, leading to differences in decomposition products within the soil [18]. These products can then directly or indirectly alter community composition and/or activity of functional proteins via substrate availability or the chemical environment. Further, in a side-by-side comparison of human and pig decomposition at the same location, soil pH increased under pigs, but decreased under humans [18]. Altered pH and soil chemistry could result in different functions and gene expression in decomposition-impacted soils. Many triacylglycerol lipases have a pH optimum that is neutral to basic [32–34], so cells may be decreasing expression under acidic conditions in human decomposition soils. Availability of lipid species and changes to pH may select for taxa that favor these substrates/pH conditions; for example, Mason et al. (2022) [12] showed a relationship between the abundance of the fungal taxa *Saccharomycetes* and antemortem body mass index (BMI) due to relative proportions of fat and muscle tissue.

967 Evidence for phased denitrification and nitrification

968
969 The human body is a concentrated source of nitrogen that is released into the sur-
970 rounding soil during decomposition. Expression of common marker genes for nitrogen
971 cycling was altered in decomposition soil and suggested nitrogen transformations
972 during human decomposition are driven by soil oxygen concentrations with hydroxy-
973 lamine as an important intermediate. We observed low or reduced expression of the
974 nitrification genes *nrrA* and *amoA* between days 12 and 86, during a period when
975 oxygen was reduced to 39% - 85%. This was concomitant with an accumulation of
976 ammonium, which reached a maximum on day 12, and low nitrate indicating that nitrifi-
977 cation was inhibited. This period of reduced soil oxygen constraining nitrification
978 was also described in a decomposition experiment with beaver (*Castor canadensis*)
979 carcasses Keenan et al. (2018) [8].
980
981

982
983 We observed increased gene expression for the enzyme hydroxylamine dehydrogenase
984 (HAO) at day 86 while oxygen was reduced (~85%). This corresponded to simultane-
985 ous increases in expression of genes encoding subunits of nitric oxide reductase (*norB*)
986 and nitrous oxide reductase (*nosZ*). Traditionally HAO has been thought to process
987 hydroxylamine to nitrite during nitrification, while nitric oxide reductase and nitrous
988 oxide reductase are enzymes involved in the last two steps of denitrification converting
989 nitric oxide (NO) to dinitrogen gas (N₂). However, recent work suggested hydroxy-
990 lamine can be converted to nitric oxide (NO), and can interact with multiple phases
991 of the nitrogen cycle [35]. Even though *amoA* expression was shown to decrease dur-
992 ing reduced oxygen conditions, *amoA* transcripts were still present and likely able
993 to convert ammonium to hydroxylamine as soil oxygen was not completely depleted
994 during decomposition. Additionally, a previous study reported that the growth of the
995 ammonia oxidizing bacteria *Nitrosomonas europaea* under anoxic conditions lead to
996 accumulation of hydroxylamine in a chemostat bioreactor [36], suggesting anaerobic
997
998
999
1000
1001
1002
1003
1004
1005
1006
1007
1008
1009
1010
1011
1012

ammonium oxidation (anammox) may also be occurring in decomposition soils. However, we did not observe increases in *nirK* expression, which might suggest conversion of nitrite to NO for use in the anammox pathway. NO produced via HAO activity may be used for anammox in these soils; however, the role of hydroxylamine as an intermediate in anammox is still debated [35]. Therefore, our current hypothesis is that hydroxylamine accumulates under anaerobic conditions during decomposition, which can then be converted to NO by HAO. This NO would then be present for anaerobic denitrifying bacteria to convert to nitrous oxide (N₂O) by nitric oxide reductase and finally to N₂ by nitrous oxide reductase. Keenan et al. (2018) [8] noted a brief increase in N₂O emissions during beaver carcass decomposition, which suggests denitrification was occurring during this phase of reduced soil oxygen concentrations.

As soils fully reoxygenated by day 168, we observed increased expression of genes encoding enzymes involved in aerobic nitrification, *amoA* and *nxrR*. Nitrification is an oxygen-dependent process which would convert accumulated ammonium to nitrate; the increase in nitrate concentrations may then serve as a substrate for denitrification. We observed increased expression of marker genes encoding all four enzymes in the complete dissimilatory denitrification pathway (*narG*, *nirK*, *norB*, and *nosZ*) at day 376. Increased expression of nitrification and denitrification marker genes is consistent with the accumulation of nitrite, nitrate, and N₂O after oxygen is reintroduced to soils described in Keenan et al. (2018) [3, 8]. Together, gene expression patterns in our study provide further insight into nitrogen transformations in during vertebrate decomposition, suggesting an important role of hydroxylamine.

Increased expression of bile salt hydrolases

Sulfur is present in various organic molecules, including taurine, a sulfur- and nitrogen-rich compound involved in bile acid formation [22]. Taurine in the human body can be absorbed from the diet or synthesized in the liver [37]. However, taurine is also

1059 produced as a byproduct of the deconjugation of bile salts via bile salt hydrolases
 1060 (BSHs) present in the anaerobic gut taxa *Lactobacillus* and *Clostridium* [22]. We
 1061 observed increased expression of genes encoding BSH enzymes between days 12 and 86.
 1062
 1063 Given that increased expression of BSH genes corresponded to the beginning of active
 1064 decomposition, when decomposition products were observed to enter the soil, and the
 1065 period of reduced dissolved oxygen in our study, it is likely that taurine accumulation
 1066 is the result of BSH enzyme activity by anaerobic microorganisms. While we did
 1067 not measure taurine concentrations in the present study, our results correspond to
 1068 previous decomposition studies that report accumulation of taurine in various organs
 1069 and body regions [38–40] and soils [18, 41] during decomposition via metabolomics,
 1070 and increased relative abundance of *Clostridium* and *Lactobacillus* within the body
 1071 [42–44] and in decomposition soils [20] via DNA sequencing methods, including in
 1072 these soils [13].
 1073

1081 Taurine can be metabolised through desulfurization via the α -ketoglutarate-dependent
 1082 enzyme taurine dioxygenase (TauD). Specifically, this enzyme, encoded by the gene
 1083 *tauD*, converts 2-oxoglutarate and taurine to produce aminoacetaldehyde, succinate,
 1084 sulfite, and CO₂ [45]. Succinate and sulfite from this reaction can then be used for
 1085 the citric acid cycle and sulfur metabolism, respectively. Given increased BSH expres-
 1086 sion in our study and reported taurine accumulation in others, we would expect
 1087 taurine to be present for microbial metabolism by TauD. However, we observed
 1088 a general decrease in *tauD* expression between days 12 through 376. This trend
 1089 was driven by reduced expression of *tauD* transcripts associated with *Proteobacteria*,
 1090 *Gammaproteobacteria*, and *Actinobacteria* whose relative abundance have been shown
 1091 to remain consistent or increase during human decomposition [20], suggesting that
 1092 *tauD* expression is downregulated under decomposition conditions. However, we noted
 1093 that expression of *tauD* genes associated with fungi and a few *Betaproteobacteria* dis-
 1094 played increased representation at day 58, corresponding to increased expression of
 1100
 1101
 1102
 1103
 1104

bile salt hydrolases (BSH) between days 12 and 86. The reduction in *tauD* expres-
 sion may be due to increased sulfur availability. We did not measure sulfur species
 in this experiment; however, others have observed increased sulfur concentrations in
 decomposition-impacted soils [3, 7, 11]. Thus, sulfur scavenging pathways such as tau-
 rine desulfurization by TauD [46], whose genes are expressed under sulfur-limiting
 conditions, likely display reduced expression under sulfur replete conditions. Addition-
 ally, taurine may be processed through other pathways. For example, taurine can be
 deaminated by taurine dehydrogenase to produce sulfite and acetyl-CoA for carbon
 metabolism [45, 47]. Overall, our results suggest that human decomposition has poten-
 tial impacts on soil sulfur biogeochemistry through deposition of inorganic (sulfate)
 and organic (sulfur-containing amino acids) sulfur compounds.

Conclusion

This study investigated soil microbial gene expression during human decomposition.
 Metatranscriptomic analysis of soils from three human individuals shows that decom-
 position impacted microbial community gene expression profiles, exhibiting functional
 shifts over one year. This included altered expression of genes involved in lipid, N
 and S metabolism as microbes processed the nutrient-rich tissues of the human body.
 Additionally, we noted that functionality within decomposition-impacted soils was
 still affected after one year and had not returned to starting or background condi-
 tions. Together, these results show that vertebrate decomposition has lasting impacts
 on local soil ecosystems, including soil microbial communities. These results have
 important implications for understanding biogeochemical changes due to vertebrate
 mortality events in terrestrial ecosystems.

1151 Materials and Methods

1152

1153

1154 Study design

1155

1156 In February 2018, three deceased male human subjects (hereafter, “donors”) were
1157 placed supine on the soil surface at the University of Tennessee Anthropology Research
1158 Facility (ARF) and allowed to decompose. Located in Knoxville, TN (35° 56’ 28” N,
1159 83° 56’ 25” W) the ARF is a roughly 2-acre outdoor facility dedicated to studying
1160 human decomposition [48]. The soils at the ARF are comprised of the Loyston-Talbott-
1161 Rock outcrop (LtD) and Coghill-Corryton (CcD) complexes. LtD soils are a silty clay
1162 loam and channery clay overlaying lithic bedrock, while CcD soils are comprised of
1163 clay from weathered quartz limestone [13, 48]. A site that had not been previously
1164 exposed to decomposition was used for this study.

1165

1166

1167 The decomposition field experiment is fully described in Taylor et al. (2024) [13].

1168

1169 Briefly, experiments were conducted in a block design, where each block consisted of

1170

1171 one decomposition site and one control site [13]. In total three blocks, *i.e.*, three donors

1172

1173 paired with three respective control sites, were included in the study. Each control site

1174

1175 was chosen in a manner to ensure their location was uphill and roughly 2 m away from

1176

1177 decomposition sites [13]. Donor internal temperatures were recorded by probes located

1178

1179 in the abdomen, while ambient air temperatures were monitored via sensors located

1180

1181 roughly 50 cm above the soil surface. Soil temperature and salinity were measured

1182

1183 with sensors placed directly underneath each individual (Decagon Devices, GS3) [13].

1184

1185 Donors ranged from 65 to 86 in age and were within 1 kg of each other with regard

1186

1187 to weight (90.7 to 91.6 kg); donor BMI varied between 27.7 to 29.6 [13].

1188

1189

1190

1191

1192

1193

1194

1195

1196

Sampling and physiochemistry

Decomposition of all subjects was observed for one year. During the one-year study period, soils were sampled at 20 timepoints chosen to correspond with morphological stages of decomposition as described by Payne (1965) [49]. Once advanced decay was reached, soils were collected at intervals of 350 accumulated degree days (ADD), calculated using ambient air temperatures, up to one year. All soil cores were taken using a 1.9 cm (3/4 inch) diameter soil auger to a depth of 16 cm. Soils were divided into two depth fractions: 0-1 cm (interface) and 1-16 cm (core) for the analyses reported in Taylor et al. (2024) [13]; the entire 0 to 16 cm core was used for this current study. Decomposition soils were taken from directly beneath the cadavers, taking care to not re-sample the same location more than once. At the time of sampling, soil dissolved oxygen was measured in triplicate using an Orion Star™ A329 pH/ISE/Conductivity/Dissolved Oxygen portable multiparameter meter (ThermoFisher) [13].

A subset of 6 study timepoints were chosen for metatranscriptomics analysis. Study days 0, 12, 58, 86, 168, and 376 were chosen as they represented distinct biogeochemical phases during decomposition (Fig. S5). Study day 0 was chosen as a baseline sample prior to cadaver placement. Study day 12 was the start of active decomposition, during the initial bloom when soil microbial activity was rapidly increasing resulting in the onset of hypoxia: soil ammonium reached maximum concentrations and soil oxygen was at minimum (approximately 39%). Study day 58 was during a climax period of sustained elevated microbial activity, characterized by high ammonium concentrations, hypoxia, maximum soil temperatures and minimum soil pH [13]. Study day 86 represented a period of declining microbial activity, declining hypoxia, and increasing nitrate concentrations. Study day 168 was chosen as nitrate was at its maximum and soil dissolved oxygen had recovered to 99%. Finally, day 376 was chosen to represent the end of the study, 1 year since cadaver placement. Each study day

1243 was represented by four soil samples for RNA extraction: one pooled control sample
1244 which was a mix of the three control locations, plus one sample from each of the three
1245 donors, yielding a total of 24 samples for this study.
1246

1247
1248
1249 Soil samples were transported to the University of Tennessee (Knoxville, TN) and
1250 processed within 24 hours of collection. Soils were homogenized by hand to remove
1251 insect larvae, roots, rocks, and other debris (> 2 mm). A subset of soils were used
1252 to measure pH, electrical conductivity (EC), and evolved CO_2 as described in Tay-
1253 lor (2024). Soil nitrogen species (NH_4^+ , NO_3^-) and total carbon (TC) and nitrogen
1254 (TN) were measured in all soil samples as described in [13]. Reported values for soil
1255 physiochemistry represent the full 16 cm core; estimated by summing interface and
1256 core values reported by Taylor et. al, (2024) [13] in 1:16 and 15:16 ratios, respectively.
1257 Control values reported here are means of the three experimental controls that were
1258 unimpacted by decomposition.
1259

1260
1261
1262 Roughly 10 g of soil was reserved for nucleic acid extraction, placed in a 4 oz. Whirl-
1263 Pak™ bag (Nasco), flash frozen in liquid nitrogen, and stored at -80°C until further
1264 analysis. Bacterial and fungal community composition was assessed via amplicon
1265 sequencing of the 16S rRNA gene and ITS2 region as described in Taylor et al. (2024).
1266

1267 **RNA Extraction and Sequencing**

1268
1269 RNA was extracted from 2 g of soil using Qiagen's RNeasy® PowerSoil® Total RNA
1270 kit. Manufacturer's instructions were followed with a few modifications. Soils became
1271 saline during decomposition; therefore, we followed the manufacturer's suggestion and
1272 incubated all extracts at -20°C following addition of solution SR4 (step 9) to decrease
1273 salt precipitation. All RNA samples were resuspended in 40 μl of Solution SR7. RNA
1274 concentrations were assessed fluorometrically using the Qubit® RNA HS assay (cat-
1275 alog no. Q32852) with 1 μl of RNA. DNA contamination was removed by DNase
1276
1277
1278
1279
1280
1281
1282
1283
1284
1285
1286
1287
1288

treating RNA extracts twice using Qiagen’s DNase Max® kit in 50 µl reactions. RNA concentrations were remeasured after DNase treatment. PCR with V4 16S rRNA gene primers [50, 51] was conducted using RNA extracts as the template to confirm removal of all DNA prior to sequencing. RNA aliquots were shipped to HudsonAlpha Discovery (Huntsville, AL) for library preparation and RNA sequencing. Dual-indexed libraries were prepared using the Illumina® Stranded Total RNA prep with ribosomal RNA depletion via ligation with Ribo-Zero Plus. Libraries were then pooled and sequenced on Illumina’s NovaSeq 6000 v4 platform, resulting in demultiplexed fastq files for each sample.

Bioinformatics

Illumina sequencing of the 24 libraries yielded a total of 5,073,476,730 reads, or 2,536,738,365 paired reads, with a mean of 105,697,432 paired reads per sample. Read quality control (QC) was conducted in KBase [52] using Trimmomatic [53]. Paired fastq files were imported to KBase through Globus. Poor quality reads were removed (4.7% of all reads), and adapters trimmed via Trimmomatic (v0.36) using default settings and the TruSeq3-PE-2 adapter file, resulting in 4,834,123,062 total reads. After QC check with FastQC, trimmed libraries were exported as fastq files from KBase through Globus. Remaining ribosomal RNA was filtered using bbmap (maxindel = 20, minid = 0.93) from the Joint Genome Institute’s (JGI) bbtools suite [54]. Filtering of ribosomal RNA further removed 7.3% of reads, leaving 4,479,804,360 reads for assembly. Following this step, all non-ribosomal reads from all 24 samples were merged into one file. Reads were then co-assembled into contigs using the de novo assembler MEGAHIT (v1.2.9) [55] (−12 −k-min 23, −k-max 123, −k-step 10).

Gene identification and annotation from co-assembled contigs was performed using Prodigal [56] and eggNOG mapper [57], respectively. Briefly, the DNA fasta containing all contigs was submitted to Prodigal (v2.6.3) for protein coding gene predication

for a meta-sample (-p meta -f gff). After co-assembly, a total of 6,257,674 gene calls were identified by Prodigal. Next, predicated genes were functionally and taxonomically annotated using eggNOG mapper (v2.1.6) using basic settings to perform a diamond blastp search [58]. From this, 1,048,573 proteins were annotated by eggNOG-mapper (16.7%). Most of the annotated proteins were taxonomically annotated as bacteria (91.3%), followed by eukaryotes (7.6 %), and archaea (0.81 %). Of the 7.6% of eukaryotic proteins, 64.4% (4.9% of all proteins) were annotated as fungi. For this study, genes of interest included all bacterial, archaeal, and fungal proteins, therefore all non-fungal eukaryotic proteins (32,004) were removed prior to downstream analysis. Transcript counts for all genes of interest were obtained by mapping reads from each respective sample to genes of interest obtained from co-assembly using QIAGEN CLC Genomics Workbench 20.0 (<https://digitalinsights.qiagen.com/>). The percent of reads mapped to genes of interest ranged from 21% to 38% between samples, with an average of 31% reads mapped. Gene counts were then combined in a single file and used for downstream analyses in R.

1360

1361 Differential Expression

1362

Transcript counts from all samples were combined in a single workable data file and imported into R for differential expression analysis using the R packages edgeR [59] and limma [60] following a modified pipeline by Phipson et al. (2020) [61]. The transcript count table was imported into R and converted to a DGEList object. Genes without sufficient counts for statistical analysis were removed to increase power using the edgeR function filterByExpr(), using study day as the comparison group.

1373

Raw counts were then log2 normalized and gene expression profiles compared via multidimensional scaling (MDS) and hierarchical clustering. Multidimensional scaling (MDS) was conducted using plotMDS() from the limma package to assess differences between samples. MDS values were extracted from the MDS object, and the first two

1380

dimensions plotted using ggplot2 [62]. We also assessed the relationship between gene expression profiles and changes in the soil environment using canonical correspondence analysis (CCA). Environmental variables of interest included decomposition time in accumulated degree hours (ADH) based on ambient temperatures, ADH based on internal gut temperatures, ADH based on soil temperatures, gravimetric moisture, pH, electrical conductivity (EC), dissolved oxygen (DO), CO₂ (μmol gdw⁻¹), NH₄ (mg gdw⁻¹), NO₃ (mg gdw⁻¹), N %, C %, and CN ratio. First, permutational multivariate analysis of variance (PERMANOVA) with adonis() (vegan v2.6.7) [63] was used to identify significant soil parameters. Then the vegan functions cca() and scores() were applied to run the CCA and extract scores, respectively. Scores for the first two dimension were plotted using ggplot2, with loadings extracted from the CCA biplot.

For differential expression analysis, raw filtered reads were normalized using edgeR's trimmed mean of M values (TMM) normalization using the function calcNormFactors(). TMM normalized reads were then log2 transformed using limma's voom() and differential expression assessed. Empirical Bayes shrinkage was used correct to p-values for false discovery rates. The topmost up and down regulated genes for each comparison, determined by log2 fold change and adjusted p-values, were then reported. Expression of certain genes were assessed after performing transcripts per million (TPM) normalization and statistical analyses with a combination of analysis of variance (ANOVA) and post-hoc Tukey tests. ANOVA across all timepoints were applied to hierarchical linear mixed effects models to account for repeated sampling within each donor block.

Availability of data and materials

Raw RNA sequence files from the Illumina Novaseq are available at the National Center for Biotechnology Information's (NCBI) Sequence Read Archive (SRA) as a part

1427 of [BioProject PRJNA1066312](#) under BioSample accession numbers SAMN45195141-
1428 SAMN45195164. Additional datasets supporting the conclusions of this article are
1429 available on [GitHub](#). Scripts containing code for all analyses and to generate figures
1430 are available on [GitHub](#).
1431
1432
1433
1434

1435 Acknowledgements

1436
1437 We would like to thank the Forensic Anthropology Center at the University of
1438 Tennessee-Knoxville for their help in setting up field experiments. We would like to
1439 thank Mary Davis for her help in managing the field site and helping to obtain donors
1440 for this work. This research was funded by a National Institute of Justice Award
1441 (DOJ-NIJ-2017-R2-CX-0008) to LST and JMD.
1442
1443
1444
1445
1446

1447 References

- 1448
1449
1450 [1] Benninger, L. A., Carter, D. O. & Forbes, S. L. The biochemical alteration of soil
1451 beneath a decomposing carcass. *Forensic Science International* **180**, 70–5 (2008).
1452
1453
1454 [2] Towne, E. G. Prairie vegetation and soil nutrient responses to ungulate carcasses.
1455 *Oecologia* **122**, 232–239 (2000).
1456
1457
1458 [3] DeBruyn, J. M., Keenan, S. W. & Taylor, L. S. From carrion to soil: microbial
1459 recycling of animal carcasses. *Trends in Microbiology* **33**, 194–207 (2025).
1460
1461
1462 [4] Parmenter, R. R. & MacMahon, J. A. Carrion decomposition and nutrient cycling
1463 in a semiarid shrub–steppe ecosystem. *Ecological Monographs* **79**, 637–661 (2009).
1464
1465
1466 [5] Macdonald, B. C. T. *et al.* Carrion decomposition causes large and lasting effects
1467 on soil amino acid and peptide flux. *Soil Biology and Biochemistry* **69**, 132–140
1468 (2014).
1469
1470
1471
1472

- [6] Bump, J. K. *et al.* Ungulate carcasses perforate ecological filters and create biogeochemical hotspots in forest herbaceous layers allowing trees a competitive advantage. *Ecosystems* **12**, 996–1007 (2009).
- [7] Aitkenhead-Peterson, J. A., Owings, C. G., Alexander, M. B., Larison, N. & Bytheway, J. A. Mapping the lateral extent of human cadaver decomposition with soil chemistry. *Forensic Science International* **216**, 127–34 (2012).
- [8] Keenan, S. W., Schaeffer, S. M., Jin, V. L. & DeBruyn, J. M. Mortality hotspots: nitrogen cycling in forest soils during vertebrate decomposition. *Soil Biology and Biochemistry* **121**, 165–176 (2018).
- [9] Fancher, J. P. *et al.* An evaluation of soil chemistry in human cadaver decomposition islands: Potential for estimating postmortem interval (PMI). *Forensic Science International* **279**, 130–139 (2017).
- [10] Quaggiotto, M.-M., Evans, M. J., Higgins, A., Strong, C. & Barton, P. S. Dynamic soil nutrient and moisture changes under decomposing vertebrate carcasses. *Biogeochemistry* **146**, 71–82 (2019).
- [11] Taylor, L. S. *et al.* Soil elemental changes during human decomposition. *PLoS ONE* **18**, 1–24 (2023). Publisher: Public Library of Science.
- [12] Mason, A. R. *et al.* Body mass index (BMI) impacts soil chemical and microbial response to human decomposition. *mSphere* e0032522 (2022).
- [13] Taylor, L. S. *et al.* Transient hypoxia drives soil microbial community dynamics and biogeochemistry during human decomposition. *FEMS Microbiology Ecology* **100**, fae119 (2024).

1519 [14] Keenan, S. W., Emmons, A. L. & DeBruyn, J. M. Microbial community coa-
1520
1521 lescence and nitrogen cycling in simulated mortality decomposition hotspots.
1522 *Ecological Processes* **12**, 45 (2023).
1523
1524
1525 [15] Mason, A. R., Taylor, L. S. & DeBruyn, J. M. Microbial ecology of vertebrate
1526
1527 decomposition in terrestrial ecosystems. *FEMS Microbiology Ecology* **99**, fiad006
1528 (2023).
1529
1530
1531 [16] Burcham, Z. M. *et al.* Total RNA analysis of bacterial community structural
1532
1533 and functional shifts throughout vertebrate decomposition. *Journal of Forensic*
1534 *Sciences* **64**, 1707–1719 (2019).
1535
1536
1537 [17] Ashe, E. C., Comeau, A. M., Zejdlik, K. & O’Connell, S. P. Characterization of
1538
1539 bacterial community dynamics of the human mouth throughout decomposition
1540 via metagenomic, metatranscriptomic, and culturing techniques. *Frontiers in*
1541 *Microbiology* **12**, 689493 (2021).
1542
1543
1544 [18] DeBruyn, J. M. *et al.* Comparative decomposition of humans and pigs: soil biogeo-
1545
1546 chemistry, microbial activity and metabolomic profiles. *Frontiers in Microbiology*
1547 **11**, 608856 (2021).
1548
1549
1550 [19] Howard, G. T., Duos, B. & Watson-Horzelski, E. J. Characterization of the
1551
1552 soil microbial community associated with the decomposition of a swine carcass.
1553 *International Biodeterioration & Biodegradation* **64**, 300–304 (2010).
1554
1555
1556 [20] Cobaugh, K. L., Schaeffer, S. M. & DeBruyn, J. M. Functional and structural
1557
1558 succession of soil microbial communities below decomposing human cadavers.
1559 *Plos One* **10**, e0130201 (2015).
1560
1561
1562 [21] Singh, B. *et al.* Temporal and spatial impact of human cadaver decomposition
1563
1564 on soil bacterial and arthropod community structure and function. *Frontiers in*

<i>Microbiology</i> 8 , 2616 (2018).	1565
	1566
[22] Urdaneta, V. & Casadesús, J. Interactions between bacteria and bile salts in the	1567
gastrointestinal and hepatobiliary tracts. <i>Frontiers in Medicine</i> 4 (2017).	1568
	1569
	1570
[23] van der Wal, A., Geydan, T. D., Kuyper, T. W. & de Boer, W. A thready affair:	1571
linking fungal diversity and community dynamics to terrestrial decomposition	1572
processes. <i>FEMS Microbiology Reviews</i> 37 , 477–494 (2013).	1573
	1574
	1575
	1576
[24] Essington, M. E. <i>Soil and water chemistry: an integrative approach</i> (CRC press,	1577
2015).	1578
	1579
	1580
	1581
[25] Peng, J., Wegner, C.-E. & Liesack, W. Short-term exposure of paddy soil micro-	1582
bial communities to salt stress triggers different transcriptional responses of key	1583
taxonomic groups. <i>Frontiers in Microbiology</i> 8 (2017).	1584
	1585
	1586
[26] Pandit, A. S. <i>et al.</i> A snapshot of microbial communities from the Kutch: one of	1587
the largest salt deserts in the World. <i>Extremophiles</i> 19 , 973–987 (2015).	1588
	1589
	1590
	1591
[27] Metcalf, J. L. <i>et al.</i> Microbial community assembly and metabolic function during	1592
mammalian corpse decomposition. <i>Science</i> 351 , 158–62 (2016).	1593
	1594
	1595
[28] Fu, X. <i>et al.</i> Fungal succession during mammalian cadaver decomposition and	1596
potential forensic implications. <i>Scientific Reports</i> 9 , 12907 (2019).	1597
	1598
	1599
[29] Dujon, B. <i>et al.</i> Genome evolution in yeasts. <i>Nature</i> 430 , 35–44 (2004).	1600
	1601
	1602
[30] Haridas, S. <i>et al.</i> The genome and transcriptome of the pine saprophyte <i>Ophios-</i>	1603
<i>toma piceae</i> , and a comparison with the bark beetle-associated pine pathogen	1604
<i>textitGrosmannia clavigera</i> . <i>BMC Genomics</i> 14 , 373 (2013).	1605
	1606
	1607
	1608
	1609
	1610

1611 [31] Notter, S. J., Stuart, B. H., Rowe, R. & Langlois, N. The initial changes of fat
1612 deposits during the decomposition of human and pig remains. *Journal of Forensic*
1613 *Sciences* **54**, 195–201 (2009).
1614
1615
1616
1617 [32] Kok, R. G. *et al.* Characterization of the extracellular lipase, LipA, of *Acineto-*
1618 *bacter calcoaceticus* BD413 and sequence analysis of the cloned structural gene.
1619 *Molecular Microbiology* **15**, 803–818 (1995).
1620
1621
1622
1623 [33] Hasan, F., Shah, A. A. & Hameed, A. Influence of culture conditions on lipase
1624 production by *Bacillus* sp. FH5. *Annals of Microbiology* **56**, 247–252 (2006).
1625
1626
1627 [34] Zouaoui, B. & Bouziane, A. Production, optimization and characterization of
1628 the lipase from *Pseudomonas aeruginosa*. *Romanian Biotechnological Letters* **17**,
1629 7187–7193 (2012).
1630
1631
1632
1633 [35] Soler-Jofra, A., Pérez, J. & van Loosdrecht, M. C. M. Hydroxylamine and the
1634 nitrogen cycle: A review. *Water Research* **190**, 116723 (2021).
1635
1636
1637 [36] Yu, R., Perez-Garcia, O., Lu, H. & Chandran, K. *Nitrosomonas europaea* adapta-
1638 tion to anoxic-oxic cycling: Insights from transcription analysis, proteomics and
1639 metabolic network modeling. *Science of the Total Environment* **615**, 1566–1573
1640 (2018).
1641
1642
1643
1644 [37] Seidel, U., Huebbe, P. & Rimbach, G. Taurine: A regulator of cellular redox
1645 homeostasis and skeletal muscle function. *Molecular Nutrition & Food Research*
1646 **63**, 1800569 (2019).
1647
1648
1649
1650 [38] Mora-Ortiz, M., Trichard, M., Oregioni, A. & Claus, S. P. Thanatometabolomics:
1651 introducing NMR-based metabolomics to identify metabolic biomarkers of the
1652 time of death. *Metabolomics* **15**, 37 (2019).
1653
1654
1655
1656

- [39] Locci, E. *et al.* A ^1H NMR metabolomic approach for the estimation of the time since death using aqueous humour: an animal model. *Metabolomics* **15**, 76 (2019).
- [40] Zelentsova, E. A. *et al.* Post-mortem changes in the metabolomic compositions of rabbit blood, aqueous and vitreous humors. *Metabolomics* **12**, 172 (2016).
- [41] Hoeland, K. M. *Investigating the potential of postmortem metabolomics in mammalian decomposition studies in outdoor settings*. Ph.D. thesis, University of Tennessee-Knoxville, https://trace.tennessee.edu/utk_graddiss/7000 (2021).
- [42] Javan, G. T. *et al.* Human thanatobiome succession and time since death. *Scientific Reports* **6**, 29598 (2016).
- [43] Javan, G. T., Finley, S. J., Smith, T., Miller, J. & Wilkinson, J. E. Cadaver thanatobiome signatures: the ubiquitous nature of *Clostridium* species in human decomposition. *Frontiers in Microbiology* **8**, 2096 (2017).
- [44] DeBruyn, J. M. & Hauther, K. A. Postmortem succession of gut microbial communities in deceased human subjects. *PeerJ* **5**, e3437 (2017).
- [45] Cook, A. M. & Denger, K. *Metabolism of taurine in microorganisms*, 3–13 (2006).
- [46] Kertesz, M. A. Riding the sulfur cycle – metabolism of sulfonates and sulfate esters in Gram-negative bacteria. *FEMS Microbiology Reviews* **24**, 135–175 (2000).
- [47] Brüggemann, C., Denger, K., Cook, A. M. & Ruff, J. Enzymes and genes of taurine and isethionate dissimilation in *Paracoccus denitrificans*. *Microbiology* **150**, 805–816 (2004).
- [48] Keenan, S. W. *et al.* Spatial impacts of a multi-individual grave on microbial and microfaunal communities and soil biogeochemistry. *PLoS One* **13**, e0208845

1703 (2018).
1704
1705 [49] Payne, J. A. A summer carrion study of the baby pig *Sus Scrofa* linnaeus. *Ecology*
1706 **46**, 592–602 (1965).
1707
1708
1709 [50] Apprill, A., McNally, S., Parsons, R. & Weber, L. Minor revision to V4 region SSU
1710 rRNA 806R gene primer greatly increases detection of SAR11 bacterioplankton.
1711 *Aquatic Microbial Ecology* **75**, 129–137 (2015).
1712
1713
1714 [51] Parada, A. E., Needham, D. M. & Fuhrman, J. A. Every base matters: assessing
1715 small subunit rRNA primers for marine microbiomes with mock communities,
1716 time series and global field samples. *Environmental Microbiology* **18**, 1403–14
1717 (2016).
1718
1719
1720 [52] Arkin, A. P. *et al.* KBase: The United States Department of Energy Systems
1721 Biology Knowledgebase. *Nature Biotechnology* **36**, 566–569 (2018).
1722
1723 [53] Bolger, A. M., Lohse, M. & Usadel, B. Trimmomatic: a flexible trimmer for
1724 Illumina sequence data. *Bioinformatics* **30**, 2114–2120 (2014).
1725
1726
1727 [54] Bushnell, B. BBTools software package (2014).
1728
1729 [55] Li, D., Liu, C.-M., Luo, R., Sadakane, K. & Lam, T.-W. MEGAHIT: an ultra-fast
1730 single-node solution for large and complex metagenomics assembly via succinct
1731 de Bruijn graph. *Bioinformatics* **31**, 1674–1676 (2015).
1732
1733 [56] Hyatt, D. *et al.* Prodigal: prokaryotic gene recognition and translation initiation
1734 site identification. *BMC Bioinformatics* **11**, 119 (2010).
1735
1736 [57] Cantalapiedra, C. P., Hernández-Plaza, A., Letunic, I., Bork, P. & Huerta-
1737 Cepas, J. eggNOG-mapper v2: functional annotation, orthology assignments, and
1738 domain prediction at the metagenomic scale. *Molecular Biology and Evolution*
1739
1740
1741
1742
1743
1744
1745
1746
1747
1748

38 , 5825–5829 (2021).	1749
	1750
[58] Buchfink, B., Reuter, K. & Drost, H.-G. Sensitive protein alignments at tree-of-	1751
life scale using DIAMOND. <i>Nature Methods</i> 18 , 366–368 (2021).	1752
	1753
	1754
[59] Robinson, M. D., McCarthy, D. J. & Smyth, G. K. edgeR: a Bioconduc-	1755
tor package for differential expression analysis of digital gene expression data.	1756
<i>Bioinformatics</i> 26 , 139–140 (2010).	1757
	1758
	1759
	1760
[60] Smyth, G. K. in <i>limma: Linear Models for Microarray Data</i> (eds Gentleman,	1761
R., Carey, V. J., Huber, W., Irizarry, R. A. & Dudoit, S.) <i>Bioinformatics and</i>	1762
<i>Computational Biology Solutions Using R and Bioconductor</i> 397–420 (Springer	1763
New York, New York, NY, 2005).	1764
	1765
	1766
	1767
	1768
[61] Phipson, B. <i>et al.</i> Differential expression analysis (2020). URL https://combine-	1769
australia.github.io/RNAseq-R/06-rnaseq-day1.html#References .	1770
	1771
	1772
[62] Wickham, H. <i>ggplot2: Elegant Graphics for Data Analysis</i> (Springer-Verlag New	1773
York, 2016). URL https://ggplot2.tidyverse.org .	1774
	1775
	1776
	1777
[63] Oksanen, J. <i>et al.</i> <i>vegan: Community Ecology Package</i> (2024). URL https://	1778
vegandevs.github.io/vegan/ .	1779
	1780
	1781
	1782
	1783
	1784
	1785
	1786
	1787
	1788
	1789
	1790
	1791
	1792
	1793
	1794